U.S. DEPARTMENT OF COMMERCE
National Technical Information Service

PB-281 282

Hydrodynamics of Diversionary Booms

Mason and Hanger-Silas Mason Co, Inc, Leonardo, J J

Prepared for

Industrial Environmental Research Lab, Cincinnati, Ohio

Apr 78

PB 281 282

EPA-600/2-78-075
April 1978

Environmental Protection Technology Series

[illegible]

REPRODUCED BY
NATIONAL TECHNICAL
INFORMATION SERVICE
U. S. DEPARTMENT OF COMMERCE
SPRINGFIELD, VA. 22161

TECHNICAL REPORT DATA (Please read Instructions on the reverse before completing)		
1. REPORT NO. EPA-600/2-78-075	2.	3. RECIPIENT'S ACCESSION NO. PB281282
4. TITLE AND SUBTITLE Hydrodynamics of Diversionary Booms		5. REPORT DATE April 1978 issuing date 6. PERFORMING ORGANIZATION CODE
7. AUTHOR(S) William E. McCracken		8. PERFORMING ORGANIZATION REPORT NO.
9. PERFORMING ORGANIZATION NAME AND ADDRESS Mason & Hanger-Silas Mason Co., Inc. P. O. Box 117 Leonardo, New Jersey 07737		10. PROGRAM ELEMENT NO. 1BB610 11. CONTRACT/GRANT NO. 68-03-0490
12. SPONSORING AGENCY NAME AND ADDRESS Industrial Environmental Research Laboratory-Cin., OH Office of Research and Development U.S. Environmental Protection Agency Cincinnati, Ohio 45268		13. TYPE OF REPORT AND PERIOD COVERED Final 14. SPONSORING AGENCY CODE EPA/600/12
15. SUPPLEMENTARY NOTES		

16. ABSTRACT

The failure of booms to contain floating oil in currents above 0.5 m/s appears to be well established. A method suggested to surmount this limitation is to use the boom in a diversionary mode to move the oil into regions of low currents where containment and removal can be accomplished. Previous tow tests with booms deployed in a diversionary mode have shown that oil droplets are often entrained in a flow under the boom. In these tests, the booms are set at an angle to the direction of tow and do not extend entirely across the tank. Typically, the length of boom employed in these tests was 30 m. Failure of the boom to contain oil occurred near the trailing end of the boom over approximately one-third of the length of the boom.

The U.S. Environmental Protection Agency sponsored a test program at their oil and hazardous materials simulated environmental test tank (OHMSETT) to study and document the near-field hydrodynamics of the trailing end of a diversionary boom. Three-dimensional flow fields were examined visually, using dye and oil droplets with a towed underwater video system designed and built as part of the program. Turbulence intensity was simultaneously documented photographically and measured with a hot-film anemometer.

17. KEY WORDS AND DOCUMENT ANALYSIS

a. DESCRIPTORS	b. IDENTIFIERS/OPEN ENDED TERMS	c. COSATI Field/Group
Performance tests Booms (equipment) Diverting Water Pollution Oils	Spilled oil cleanup Diverting floating oil	43F 68D

18. DISTRIBUTION STATEMENT	19. SECURITY CLASS (This Report)	21. NO. OF PAGES
RELEASE TO PUBLIC	UNCLASSIFIED	57
	20. SECURITY CLASS (This page) UNCLASSIFIED	22. PRICE A04 - A01

EPA Form 2220-1 (9-73)

☆ U.S. GOVERNMENT PRINTING OFFICE: 1978-757-140/6815 Region No. 5-11

EPA-600/2-78-075
April 1978

HYDRODYNAMICS OF DIVERSIONARY BOOMS

by

William E. McCracken
Mason & Hanger-Silas Mason Co., Inc.
Leonardo, New Jersey 07737

Contract No. 68-03-0490

Project Officers

Frank J. Freestone
John S. Farlow
Oil and Hazardous Materials Spills Branch
Industrial Environmental Research Laboratory
Edison, New Jersey 08817

INDUSTRIAL ENVIRONMENTAL RESEARCH LABORATORY
OFFICE OF RESEARCH AND DEVELOPMENT
U.S. ENVIRONMENTAL PROTECTION AGENCY
CINCINNATI, OHIO 45268

ia

DISCLAIMER

This report has been reviewed by the Industrial Environmental Research Laboratory, U.S. Environmental Protection Agency, and approved for publication. Approval does not signify that the contents necessarily reflect the views and policies of the U.S. Environmental Protection Agency, nor does mention of trade names or commercial products constitute endorsement or recommendation for use nor does the failure to mention or test other commercial products indicate that other commercial products are not available or cannot perform similarly well as those mentioned.

FOREWORD

When energy and material resources are extracted, processed, converted, and used, the related pollutional impacts on our environment and even on our health often require that new and more efficient pollution control methods be used. The Industrial Environmental Research Laboratory - Cincinnati (IERL-Ci) assists in developing and demonstrating new and improved methodologies that will meet these needs both efficiently and economically.

This report describes full-scale testing of the flow field around a commercial oil spill boom. Based on the results presented here, more efficient operating techniques for booms used in water currents above 0.5 m/s can be developed. The methods, results, and techniques described are of interest to those interested in specifying, using, or testing such equipment. Further information may be obtained through the Resource Extraction and Handling Division, Oil and Hazardous Materials Spills Branch, Edison, New Jersey.

David G. Stephan
Director
Industrial Environmental Research Laboratory
Cincinnati

ABSTRACT

The failure of booms to contain floating oil in currents above 0.5 m/s appears to be well established. A method suggested to surmount this limitation is to use the boom in a diversionary mode to move the oil into regions of low currents where containment and removal can be accomplished. Previous tow tests with booms deployed in a diversionary mode have shown that oil droplets are often entrained in a flow under the boom. In these tests, the booms are set at an angle to the direction of tow and do not extend entirely across the tank. Typically, the length of boom employed in these tests was 30 m. Failure of the boom to contain oil occurred near the trailing end of the boom over approximately one-third of the length of the boom.

The U.S. Environmental Protection Agency sponsored a test program at their oil and hazardous materials simulated environmental test tank (OHMSETT) to study and document the near-field hydrodynamics of the trailing end of a diversionary boom. Three-dimensional flow fields were examined visually, using dye and oil droplets with a towed underwater video system designed and built as part of the program. Turbulence intensity was simultaneously documented photographically and measured with a hot-film anemometer.

This report was submitted in fulfillment of Contract No. 68-03-0490, Job Order No. 21, by Mason & Hanger-Silas Mason Co., Inc. under the sponsorship of the U.S. Environmental Protection Agency. This report covers the period March 1976 through September 1976, and work was completed as of September 1977.

CONTENTS

Foreword iii
Abstract iii
Figures iv
Tables vi
Abbreviations and Symbols vi
Acknowledgment vii

1. Introduction and Objectives 1
2. Conclusions 5
3. Recommendations 6
4. Facility and Test Apparatus Description 7
5. Test Procedures and Results 11
6. Discussion of Results 26

References 28
Appendices

A. OHMSETT Description 30
B. Underwater Video 32
C. B.F. Goodrich Sea Boom 34
D. Test Equipment 35
E. Test Procedure for Turbulence Measurement 39
F. Presentation of Test Results 42

FIGURES

Number		Page
1	Experimental set-up	3
2	Sketch of diversionary boom test details	4
3	Video resolution chart	8
4	Video camera and turbulence probe support system . .	12
5	Accumulation and thickening of oil at the trailing end of the boom	17
6	Oil funneling effects	18
7	Schematic vector diagram of flow patterns at trailing end of diversionary boom	20
8	Schematic vector diagram of flow patterns of diversionary boom	21

TABLES

Number		Page
1	Video Documentation of Oil Diversion	14
2	Flow Visualization Results	19
3	Turbulence Test Matrix	23
4	Selected Turbulence Intensity Results	25

LIST OF ABBREVIATIONS AND SYMBOLS

ABBREVIATIONS

cm	--centimeter
cm^2/s	--centimeters squared per second
dB	--decibel
dyne/cm	--dynes per centimeter
F_C	--footcandle
ft	--feet
ft/min	--feet per minute
in	--inch
kg	--Kilogram
kg/m	--kilograms per meter
kHz	--kiloHertz
kt	--knot
lbs/ft	--pounds per foot
ln	--natural log
lx	--lux
m	--meter
mm	--millimeter
m/s	--meters per second
ms^{-1}	--meters per second
m^2/s	--meters squared per second
m^3/s	--cubic meters per second
m^3s^{-1}	--cubic meters per second
m^3	--cubic meters
mV	--millivolt
N/m	--newtons per meter
OHMSETT	--Oil and Hazardous Materials Simulated Environmental Test Tank
ppm	--parts per million
R_{Temp}	--probe sensor resistance
μm	--micron
V	--volt

SYMBOLS

E	--voltage
E_B	--bridge anemometer output voltage
E_O	--bridge anemometer output voltage at zero velocity
μ	--tow speed
Ω	--ohms
°	--degrees (angular)
°C	--degrees (Celsius) ≃ --approximately equal to

ACKNOWLEDGMENTS

Mr. Frank J. Freestone, the OHMSETT Project Officer, provided guidance and assistance throughout this project. Mr. J. Stephen Dorrler, Chief of The U.S. Environmental Protection Agency Oil Spill Technology Branch, Edison, New Jersey, also offered valuable suggestions.

Dr. Richard Hires from the Davidson Laboratory of Steven's Institute of Technology provided considerable instrumental and consulting expertise.

Mr. Richard Griffiths of the U.S. Coast Guard kindly reviewed this report and made a number of excellent suggestions.

The Naval Ship Research and Development Center, Bethesda, Maryland, loaned their underwater video camera system, which we used in the testing and refinement of our own.

The author wishes to express his appreciation to Stanley G. Keadle, Video Technician, and Sol H. Schwartz, Engineering Aide of Mason & Hanger-Silas Mason Co., Inc., for their individual contributions and suggestions with the underwater video and turbulence measurement systems operations developed at OHMSETT as part of this project.

SECTION 1

INTRODUCTION AND OBJECTIVES

BACKGROUND

Consider that a boom has a particular zone in its design that has the function of spill control. For a boom operating in the diversionary mode, the oil spill must reach this control zone and remain there long enough to be diverted into a collection zone. Water motion relative to the oil in or near the control zone has two effects: first, to cause oil droplet formation; and second, to entrain these droplets in water currents near the boom.

The primary factor that causes interfacial waves and oil entrainment is uncertain. Interfacial waves may be Kelvin-Helmholtz waves caused by flow instabilities, or they may be induced by background turbulence in the flow, which then entrains and disperses the droplets. If the turbulence that leads to droplet formation and subsequent entrainment can be adequately measured, then the ability to design and build better booms will be enhanced.

This report presents an experimental study of the flow and the entrainment of entrained oil around an oil-spill containment boom operating in the diversionary mode. Previous work has mostly dealt with booms operating in the containment mode (catenary configuration), and the importance of such dimensionless numbers as Froude, Weber, Reynolds, and Strouhal has been clearly noted (4, 8, 9). Droplets have been observed to form first from the crests of the interfacial waves of the oil slick (9).

Previous experimental work conducted at the U.S. Environmental Protection Agency (EPA) oil and hazardous materials simulated environmental test tank (OHMSETT) facility in Leonardo, New Jersey, has confirmed field experience that a significant improvement in boom performance results when a boom is operated at an angle to the current to divert the oil into quiescent zones for removal. Booms can be operated effectively in currents greater than 0.5 m/s by decreasing the angle between the boom and current. However, attempts to calculate or predict the maximum current in which a boom can be effectively used have been inaccurate because of the complexities of the problem. Observations of many documented tests at OHMSETT (6,7) indicate that diversionary boom performance is affected by the following factors:

Difficulty of maintaining a constant angle between the boom

and current--angular variation along the boom;

- Accumulation of oil against the boom and thickening (width and/or depth) of the oil envelope in the direction of oil diversion;

- Development of interfacial waves and consequent entrainment along the boom as well as normal to the current.

The purpose of this work was to document clearly the complex three-dimensional flow patterns near the boom with and without oil and to measure the intensity of turbulence upstream and downstream of the boom near the observed failure points along the boom.

The experimental test set-up is shown in Figure 1. A boom was rigged to be angled 34° to the tow direction using a special tow device for the trailing end and a tow strut attached to the traveling bridge for the leading end. In an attempt to maintain a reasonably constant angle along the boom while under tow, mooring lines were attached as shown in Figure 2. With this arrangement, three types of experiments were conducted: 1) simulated oil slick encountering the boom; 2) oil droplet and dye tracing of hydrodynamic flow patterns; and 3) turbulence measurements upstream and downstream of the boom. All experiments were documented with underwater video, above-water video, and 16-mm color motion pictures (regular and slow-motion) through the underwater windows along the tank wall.

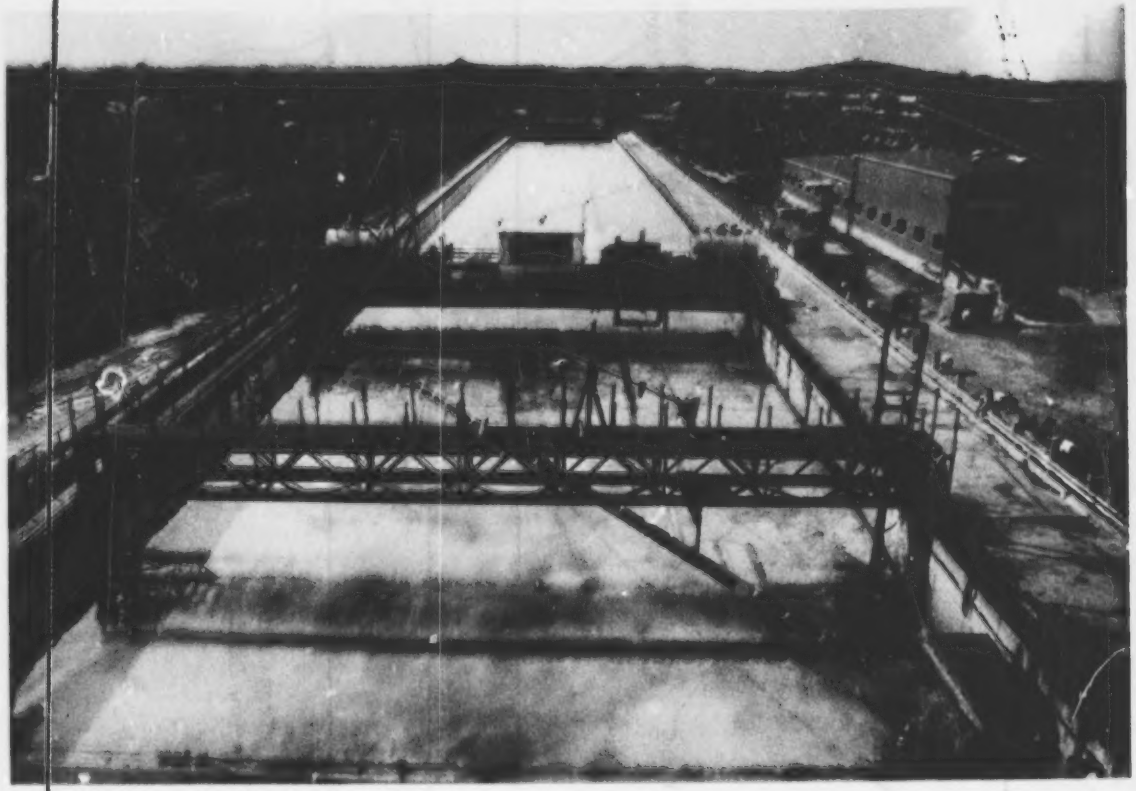

Figure 1. Experimental set-up.

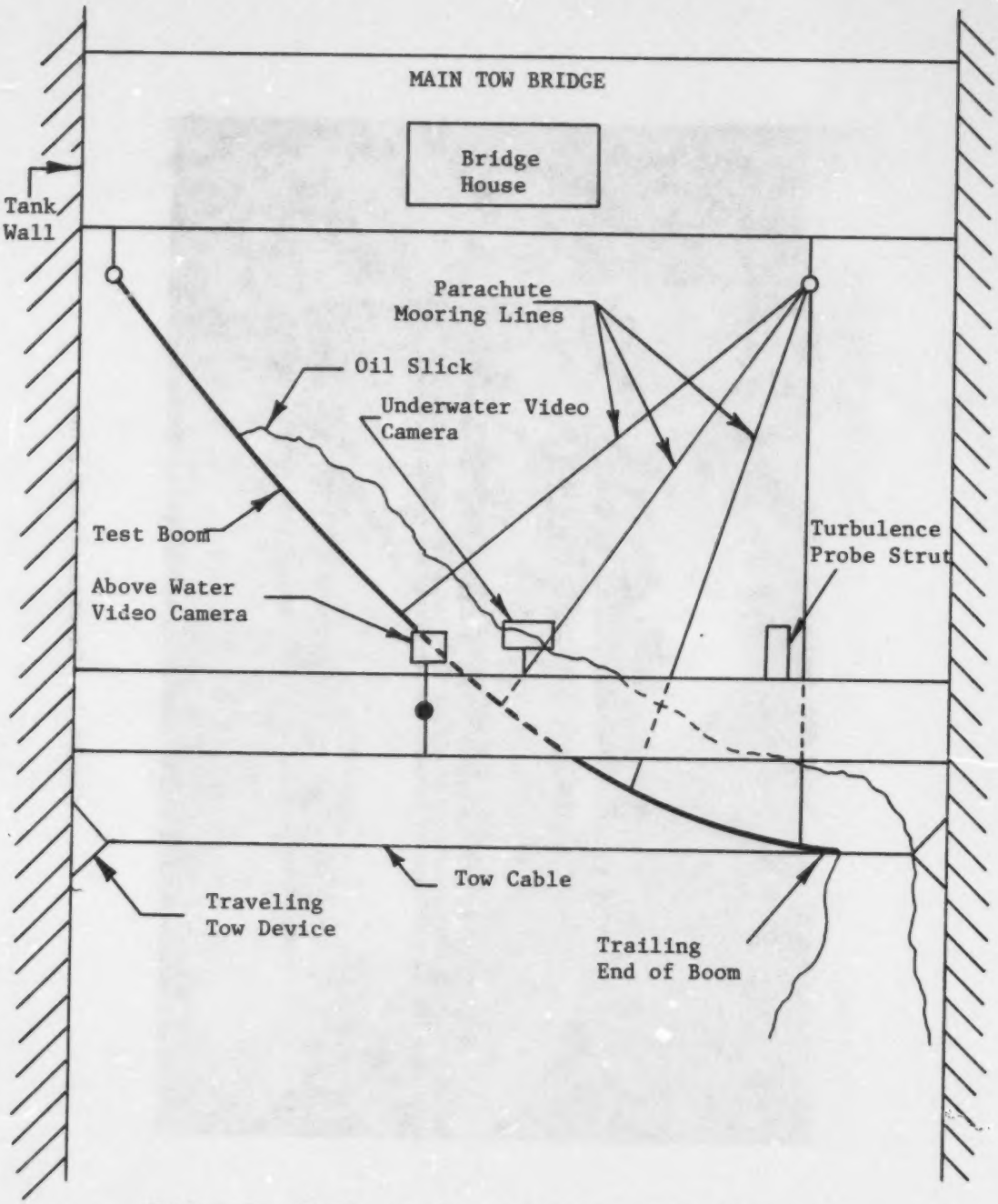

Figure 2. Sketch of diversionary boom test details.

SECTION 2

CONCLUSIONS

Through the use of newly developed turbulence measurement and underwater video capabilities, together with flow visualization techniques, certain water flow characteristics have been identified that directly affect the performance of a diversionary boom. Carefully documented data have shown that the performance of a boom angled against a current greater than 0.5 m/s (in which an oil spill is to be diverted into a collection area), cannot be easily predicted from its performance head-on against the current (catenary configuration). Streamlined rigid booms that can be moored to maintain a near constant angle against the current, with minimal near field turbulence, should demonstrate superior performance to conventional unstreamlined flexible booms.

Near-field turbulence measurements with a constant temperature, conical shaped, hot film anemometry probe indicated a marked increase in turbulence intensity from front to back of the boom at tow speeds between 0.6 and 0.8 m/s. Although localized differences in turbulence intensity were not measured either in front of or behind the boom, the underwater video camera did show vertical vortices forming in front of the boom, spaced approximately 0.30 m apart, when an oil slick was diverted along the boom at speeds above 0.8 m/s. These vortices effectively entrained the oil and directed it downward into the fast stream lines, where it was entrained and swept under the boom skirt.

Analysis of all quantitative and qualitative data indicates complex flow patterns with high turbulence intensity behind the boom and localized vortices and three-dimensional eddies both upstream and downstream of the boom. All of these flow characteristics directly affect boom stability and oil slick stability at the oil/water interface, which in turn determines the performance limitations of a diversionary boom.

SECTION 3

RECOMMENDATIONS

Analysis of the hydrodynamic data of booms should continue, both on a full scale and laboratory level. Developed flow visualization and turbulence measurement techniques should now be used to compare the near-field flow patterns of streamlined booms (low turbulence generators) and conventional booms (high turbulence generators). Quantitative measurements could then be used to correlate flow patterns with performance. These would be useful data for improving boom designs.

Turbulence data should be analyzed as completely as possible to help understand and control the complex flow patterns. Analysis of frequency spectra would permit a more detailed analysis of the data.

SECTION 4

FACILITY AND TEST APPARATUS DESCRIPTION

TEST TANK

The OHMSETT facility, located in Leonardo, New Jersey, was built specifically for testing oil and hazardous materials containment and recovery equipment (Appendix A). Waves can be generated up to 0.8 m high and 36.6 m long, and current can be simulated with a towing bridge up to 3.1 m/s. The tank can be filled with either fresh or sea water. The sea water of the Raritan Bay (salinity 20 ppt) was used during these tests.

UNDERWATER VIDEO SYSTEM

To effectively examine the three dimensional flows of water and oil around a diversionary oil spill control barrier, it was necessary to develop underwater video systems capable of resolving oil droplets entrained in the water flows around the spill control devices. The objective of the test series designed to develop this system was to define resolution and depth of field. This was to be done in a two part series: a "target" series using a resolution target, and a "bead" series using plastic beads as an oil simulant during testing.

Video signals were recorded on an IVC 700, 2.5-cm tape deck and monitored on two Sony 22.9-cm black and white receivers. The resolution chart consisted of a 0.9 x 1.2-m sheet of 1.9-cm plywood painted white (Figure 3). Gloss black vinyl tape and lettering were used to make a crossing pattern with the tape strips, varying in step from 1.9 to 0.3 cm. The board was suspended from a 10.2-cm rod of polyethylene for vertical viewing and from two rods on opposite edges for horizontal viewing.

Two camera systems were used. The Naval Ship Research and Development Center (NSRDC) provided one camera system that consisted of a vertical strut of 7.6-cm pipe with a horizontal streamlined tube approximately 0.9-m long that had a ground glass dome and rotatable mirror assembly. The housing contained a standard resolution camera. The other camera system, designed and built for EPA, consisted of a torpedo-shaped outer housing approximately 2.7-m long and was supported by a 6.1-m horizontal traversing rod held at various depths by a vertical support. Within the outer housing was an IVC 40 M 805 line, high resolution camera encased in stainless steel. The camera (which was controlled from the surface)

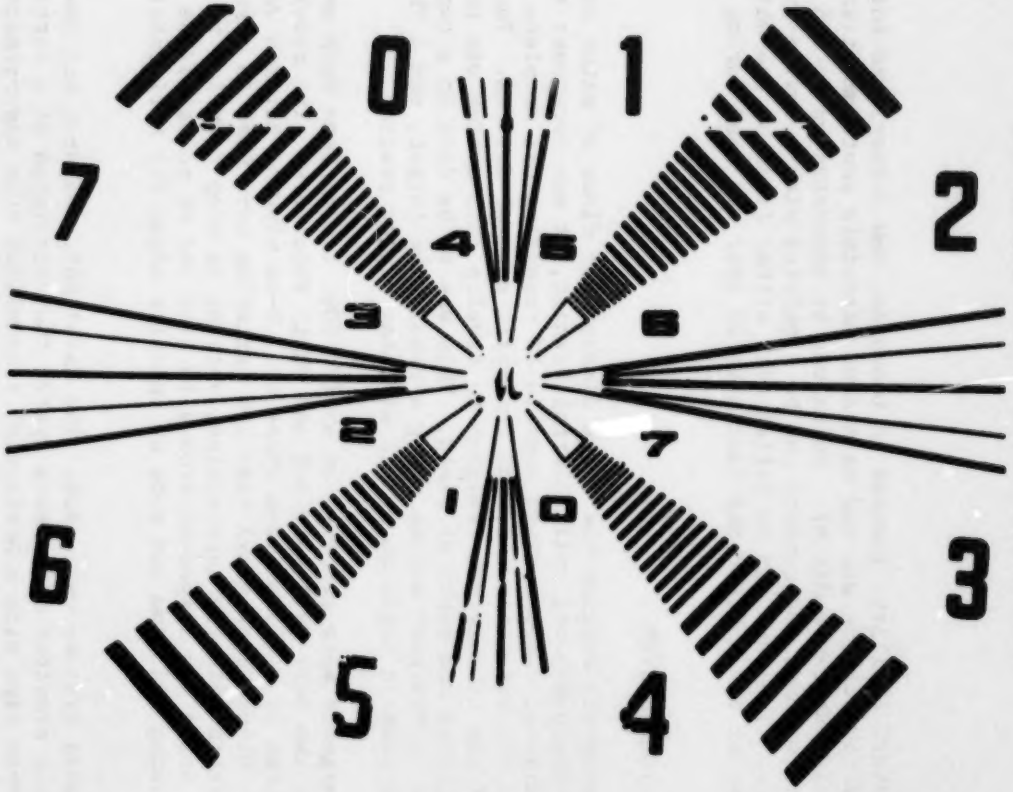

Figure 3. Video resolution chart.

looked forward into a flooded mirror compartment in which a rear surface mirror was set at 45° to look out an opening approximately 25.4 by 30.4 cm. On opposite sides of this opening and facing the target area were two Hydro LQ1000 underwater lights of 1,000 watts each.

OIL DIVERSION DOCUMENTATION TECHNIQUE

Underwater and above-water video cameras were used to document the oil slick behavior and droplet formation along the entire length of the boom (28 m). Both cameras were mounted from a towable truss that could be longitudinally positioned along the tank (see Figure 2). Both cameras were also connected to mounts that could be positioned laterally, allowing complete coverage of the boom. The boom skirt was painted white, with black numbers sequentially marking off every meter from the trailing edge to the leading edge. Likewise, white numbers were painted on the top flange of the boom. Also, a calibrated strip of aluminum was mounted horizontally from the boom freeboard member and projected outward over the oil slick along the boom to measure its width as tow speeds were varied.

FLOW VISUALIZATION TECHNIQUES

The three-dimensional flow patterns near the trailing edge of the boom were observed and documented with photo/video equipment using a water soluble dye (Red food dye #40) and several different oils as tracer elements. Various combinations of oils with specific gravities above and below 1.0 were used to develop neutrally buoyant tracers. These tracers were dyed red to enhance photographic/video documentation. Color, 16-mm motion picture films were taken at normal and slow-motion speeds for careful analysis of the flow patterns. Tracer fluids were injected upstream of the boom at various positions along the boom through three nozzles spaced 10 cm apart vertically. The upper nozzle was generally positioned within 2.5 cm of the still water surface.

TURBULENCE MEASUREMENT SYSTEM

In addition to the instrumentation listed above, it was decided to use a single axis, hot film probe for turbulence measurements. The hot wire or hot film probe is presently the most widely used measuring system for analysis of the micro-structure of turbulent gas and liquid flows.

The hot film anemometer possesses features that make it ideal for testing liquid turbulence:

- Small sensing element dimensions, hence high spatial resolution and little interference to flow.
- Brief response time as a result of small sensor mass.
- High system sensitivity.

The use of the single axis probe required an anemometer module, one linearizer, one power amplifier, a visicorder, two integrating digital voltmeters, a "tripping box," a counter, and an R.M.S. module. In addition, a second probe support had to be provided for the single axis, hot film sensor.

The electronic instrumentation devices for testing were leased from the Davidson Laboratory of Stevens Institute of Technology. The selected equipment was as follows:

- Probe--DISA 55B87 Conical Film Probe
- Electronic instrumentation--DISA 55D01 constant temperature anemometer, DISA 44D10 linearizer, DISA 55D35 RMS voltmeter, and DISA 55D25 auxiliary unit.

A complete photographic record consisting of 35-mm slides, underwater video films, and 16-mm movies was made of the testing program.

SECTION 5

TEST PROCEDURES AND RESULTS

GENERAL SET-UP

The procedures for all tests were substantially similar. The boom was positioned in a diversionary mode and connected by ropes between the main towing bridge and a light truss, both of which span the tank and travel its length (Figures 1 and 2). In an attempt to maintain a reasonably constant 34° angle along the boom while under tow, mooring lines were attached (Figure 2). With this arrangement, three types of tests were conducted: 1) oil slick encountering the boom; 2) oil droplet and dye tracing of hydrodynamic flow patterns; and 3) turbulence measurements upstream and downstream of the boom. Since the first two tests required underwater video documentation, an underwater video system was developed (Appendix B) as well as a tow strut to support it under tow (Figure 4).

OIL DIVERSION TESTS

The maximum current in which a boom can operate when angled to the current without oil loss can be estimated from its performance in the containment (catenary) mode. Knowing that oil loss in the containment mode occurs when the current normal to the boom exceeds 0.4 m/s (typical for many oils), it can be conjectured that oil loss with a boom angled to the current will occur when the component of that current normal to the boom exceeds 0.4 m/s. So for the test boom angled at 34° to the current and capable of containing oil in 0.4 m/s current, a projected maximum current in which it should divert oil without entrainment loss is 0.7 m/s. However, during an earlier test project including this boom (5), OHMSETT diversionary performance data indicated oil loss at 0.6 m/s. Oil entrainment was generally observed to occur along the trailing one-third of the boom.

Utilizing previous test data and results, it was hypothesized that there were three causes (assuming test tank effects were negligible) for this inability to attain maximum projected performance:

1) Inability to maintain an angle of ≃ 34° against the current, especially at the trailing end;

2) An accumulation of spill material being diverted all along the boom toward the trailing end, resulting in oil thickening at

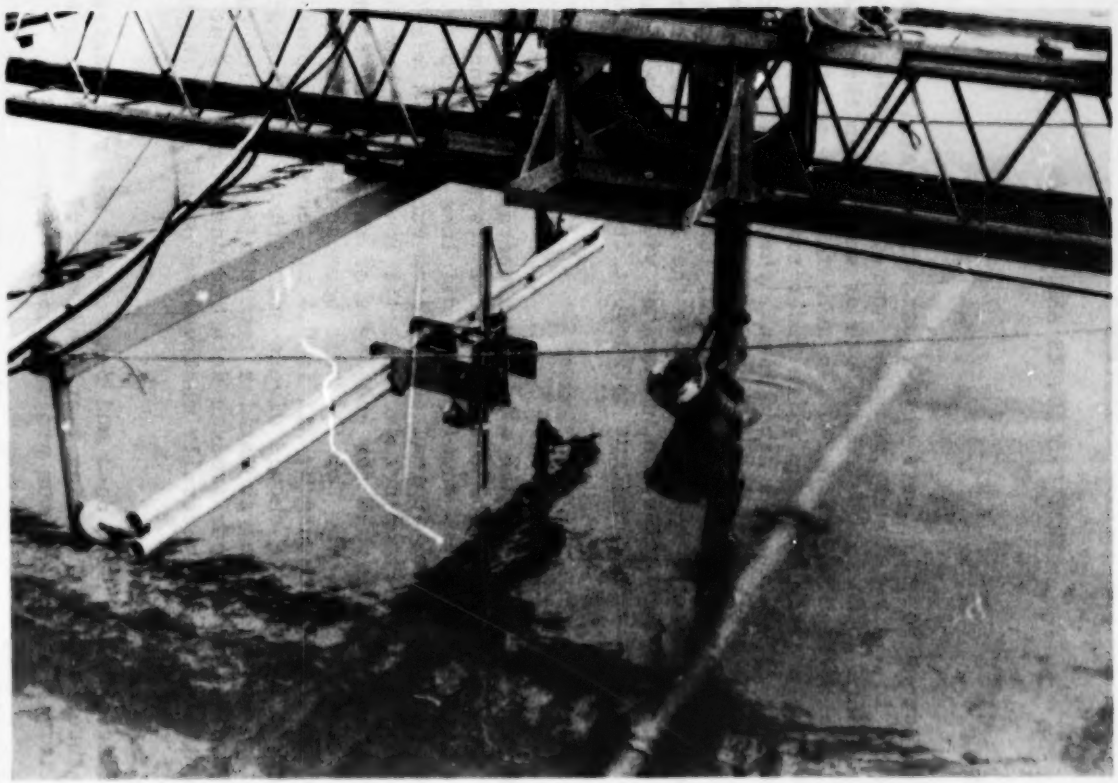

Figure 4. Video camera and turbulence probe support system.

the trailing edge and drainage losses; and

3) Complex turbulent flow patterns caused by three dimensional flow near-field of the trailing end as opposed to the predominately two dimensional flow near-field of the catenary boom apex.

To test these hypotheses, a B.F. Goodrich boom (Appendix C) was rigged and tested with oil. The test set-up was aimed toward accurate and high resolution video documentation from above and below a diversionary boom in full-scale operation under controlled test conditions. Tests were run at tow speeds of 0.6, 0.7, and 0.8 m/s in an oil slick 9 m wide, 1 mm thick and uniformly laid down at the rate of 0.4 m^3/min for 3.5 min. For ambient temperatures near 25°C, the oil properties were:

- viscosity = 1.5×10^{-4} m^2/s
- interfacial tension = 15×10^{-3} N/m
- surface tension = 30×10^{-3} N/m
- specific gravity = 0.87
- percent water = 0.2%

A test run consisted of positioning the cameras at approximately right angles to each other and viewing the horizontal plane above the boom and the underwater vertical plane along the oil side of the boom skirt. With the boom tensioned between the main tow bridge and a portable tow device at the trailing end, the tow speed was quickly brought to 0.6 m/s, the oil slick lay-down was begun, and video documentation began. As oil accumulated against the boom and built up a steady diversion rate at the trailing end, conditions were held constant for at least 15 s to accommodate full photographic coverage. Then the tow speed was increased to 0.7 m/s and 0.8 m/s in similar fashion. Duration of each test run was about 3.5 min, after which the tow systems were moved back to the starting position.

The results of this test series are tabulated in Table 1 and support the three hypotheses. Oil droplet formation was observed as far as 18 m from the trailing end of the boom, where the boom angle was between 25° and 30° at a tow speed of 0.8 m/s. Using 28° as an approximation of the boom angle, the component of tow speed (relative water motion) normal to boom is 0.38 m/s. This figure is 12% lower than the 0.43 m/s critical velocity speed for slick failure previously documented using this boom operating in the catenary configuration (5). The difference may be due to using different oils in these two tests.

Droplet size increased from about 3 mm at the 16-m mark to 25 mm at the 3-m mark with the tow speed set at 0.8 m/s. Droplet size was associated with the accumulation and thickening of the oil slick to a maximum of about 0.15 m at the trailing end of the boom as shown in

TABLE 1. VIDEO DOCUMENTATION OF OIL DIVERSION

Distance from trailing edge of boom, m	Tow speed, m/s (kts)	Boom angle, in degrees	Oil entrainment description underwater video	Oil stream width along boom, above video, m
0-3	0.6 (1.2)	---	Small amounts, small droplets	0.75 at trailing edge, 0.50 at 3 m
	0.7 (1.4)	---	Significant amounts, larger droplets of about 6 mm diameter	0.63 at trailing edge, 0.40 at 3 m
	0.8 (1.6)	60	Large amounts of oil ripping off, 18-25 mm droplets at trailing edge	0.50 at trailing edge, 0.30 at 3 m
3-7	0.6 (1.2)	---	No droplets	0.80 at 6 m mark
	0.7 (1.4)	---	Droplets begin to form, approx. 3-6 mm diameter	0.75 at 6 m mark
	0.8 (1.6)	50	High rate of droplet formation, larger size, 18 mm diameter	0.60 at 6 m mark
7-10	0.6 (1.2)	---	No droplet	0.43 at 9 m mark
	0.7 (1.4)	40	Droplets begin to form	0.50 at 9 m mark
	0.8 (1.6)	---	High rate of droplet formation	0.41 at 9 m mark

(Continued)

TABLE 1. (Continued)

Distance from trailing edge of boom, m	Tow speed, m/s	(kts)	Boom angle, in degrees	Oil entrainment description underwater video	Oil stream width along boom, above video, m
10-13	0.6	(1.2)	---	No droplets	0.43 at 12 m mark
	0.7	(1.4)	---	Very few droplets	0.38 at 12 m mark
	0.8	(1.6)	35	Nominal rate of droplet formation	0.38 at 12 m mark
13-16	0.6	(1.2)	---	No droplets	0.25 at 15 m mark
	0.7	(1.4)	---	Slight droplet formation	0.17 at 15 m mark
	0.8	(1.6)	30	Nominal rate of droplet formation (3 mm diameter)	0.12 at 15 m mark
16-24	0.6	(1.2)	---	No droplets	0.17 at 21 m mark
	0.7	(1.4)	---	No droplets	0.12 at 21 m mark
	0.8	(1.6)	25	A few detectable droplets to 18 m mark	0.12 at 21 m mark
25-28	0.6	(1.2)	---	No droplets	0.12 at 25 m mark
	0.7	(1.4)	---	No droplets	0.08 at 25 m mark
	0.8	(1.6)	15	No droplets	Cannot measure

(Figure 5). Droplets also follow along the underside of the diverting slick and grow by colliding with and contacting other droplets. The failure of oil under the boom at the trailing end and at 0.8 m/s can be described better as drainage than as entrainment. When tow speeds were increased beyond 0.8 m/s, vortices were observed that show oil funneling effects (Figure 6).

The data in Table 1, also show that as the tow speed was increased from 0.6 to 0.8 m/s, the oil slick was compressed against the boom as the "stream width" changed markedly from the 10-m mark to the trailing end of the boom. Here the boom angle was the greatest (40° → 60°). Of course, since oil is incompressible, both the oil stream depth and speed increased with distance from the upstream end of the boom, and both effectively contributed to oil loss under the boom.

FLOW VISUALIZATION TESTS

With the same general test set-up described above, several different tracer elements were tested to observe the three dimensional flow patterns near the trailing edge of the boom. Up to two tracer element injectors (described in Section 4), were used to inject tracer fluids between 2.5 and 30.0 cm beneath the water surface at tow speeds of 0.50 to 1.0 m/s. During each test run, the traced flow patterns were documented with the underwater video camera, and for selected runs, with a color 16-mm movie camera. Table 2 summarizes the test runs, and typical traces are schematically shown in Figures 7 and 8. Also, the flow visualization records were summarized in an OHMSETT-edited, unnarrated, 16-mm movie (color film and multiplexed black and white video film).

TURBULENCE MEASUREMENTS

Basically, two mechanisms exist for oil loss under a boom skirt in calm water: entrainment and drainage. For booms operating in the diversionary mode, these mechanisms have been observed to occur at about 0.65 m/s, depending on the angle between the boom and current. Drainage has been observed at the trailing edge of the boom, with entrainment at various points along the length of the boom.

Some investigators feel that entrainment is due primarily to interfacial turbulence. Instabilities form at the oil/water interface; turbulent oil waves form and droplets develop that either become entrained in the water flow under the boom or move about near the interface. Since turbulence is such an integral part of boom performance, turbulence intensity measurements were taken at various positions upstream and downstream of the boom in the near-field regions of observed failure points.

Point measurement of turbulence along the oil/water interface was not feasible with existing technology. Hot film anemometry probes, presently used for point measurements, were subject to contamination by the oil droplets that encounter the sensor element. Using the DISA 55B87 conical film probe, gross measurements of turbulence intensities

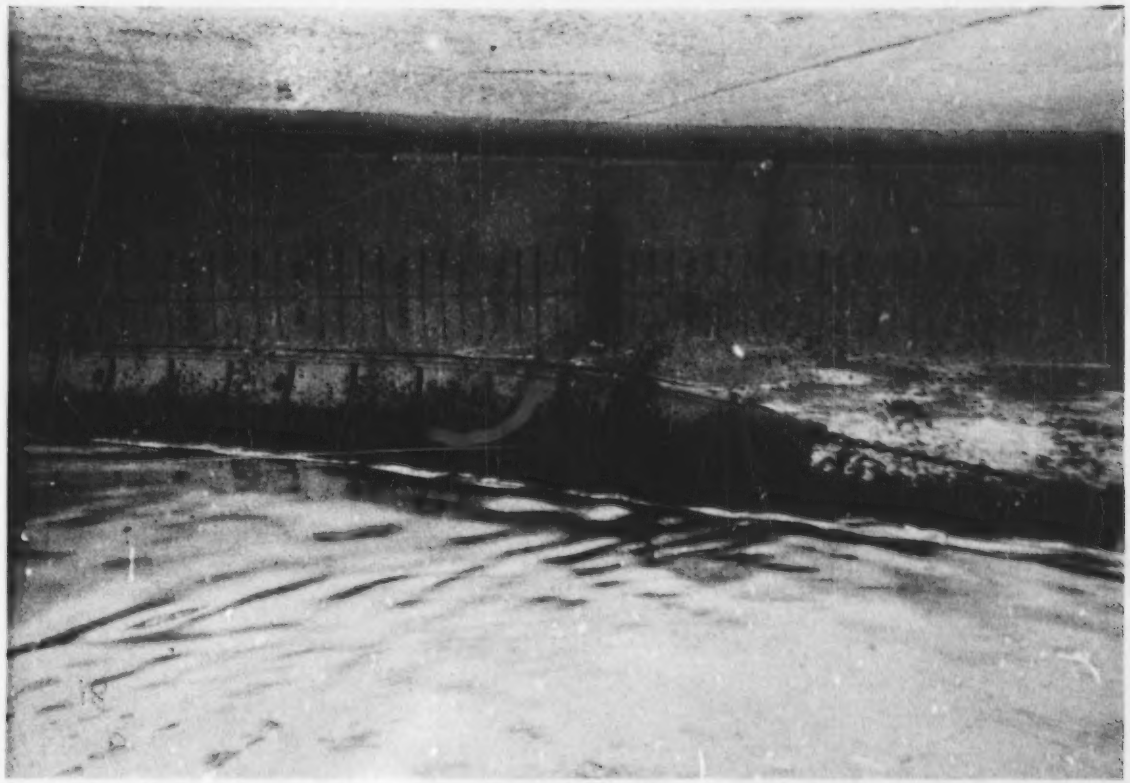

Figure 5. Accumulation and thickening of oil at the trailing end of the boom.

Figure 6. Oil funneling effects.

TABLE 2. FLOW VISUALIZATION RESULTS

Test no.	Position of nozzles, m* x	y	z	Tow speed, m/s	Tracer Fluids Type 1	SG*	Type 2	SG	Type 3	Combination ratios 1	2	Comments
1	1.8	0.60	0.30	0.50	M-100**	1.00	-----	---	------	1	---	Good trace
2	1.8	0.45	0.08	0.75	M-100	1.00	-----	---	------	1	---	Good trace
3	1.8	0.30	0.08	1.00	M-100	1.00	-----	---	------	1	---	Good trace
4	1.8	0.30	0.00	0.50	DOP***	0.98	-----	---	------	1	---	No droplets, too viscous
5	1.8	0.30	0.00	0.75	Dye	----	-----	---	------	1	---	Poor trace
6	1.8	0.15	0.00	0.50	M-120****	1.20	Octanol	0.83	Red dye	1/2	1/2	Good trace
7	1.8	0.15	0.00	0.75	DOP	0.98	Diesel	0.85	Red dye	2/3	1/3	Good trace
8	1.8	0.15	0.00	0.75	M-120	1.20	Octanol	0.83	Red dye	1/2	1/2	Good trace

*Use the axes key given with Table 4.
**Meriam 100 gage oil
***Dioctyl phthalate
****Meriam 120 gage oil

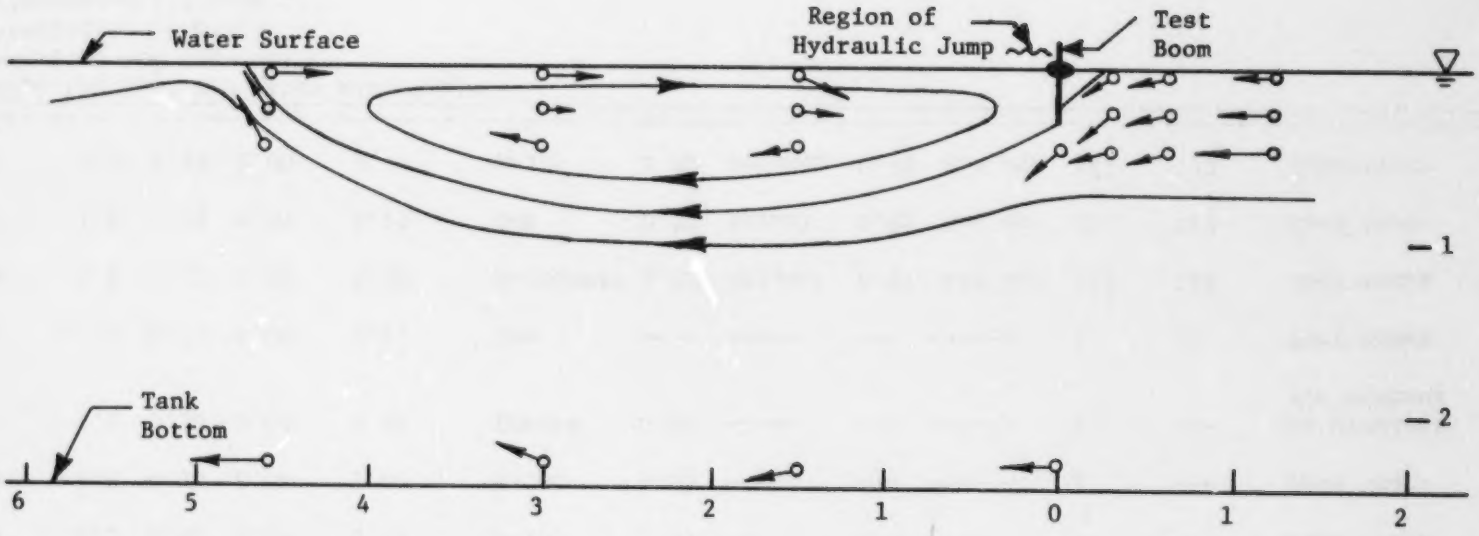

Figure 7. Schematic vector diagram of flow patterns at trailing end of diversionary boom (section view). All measurements in meters.

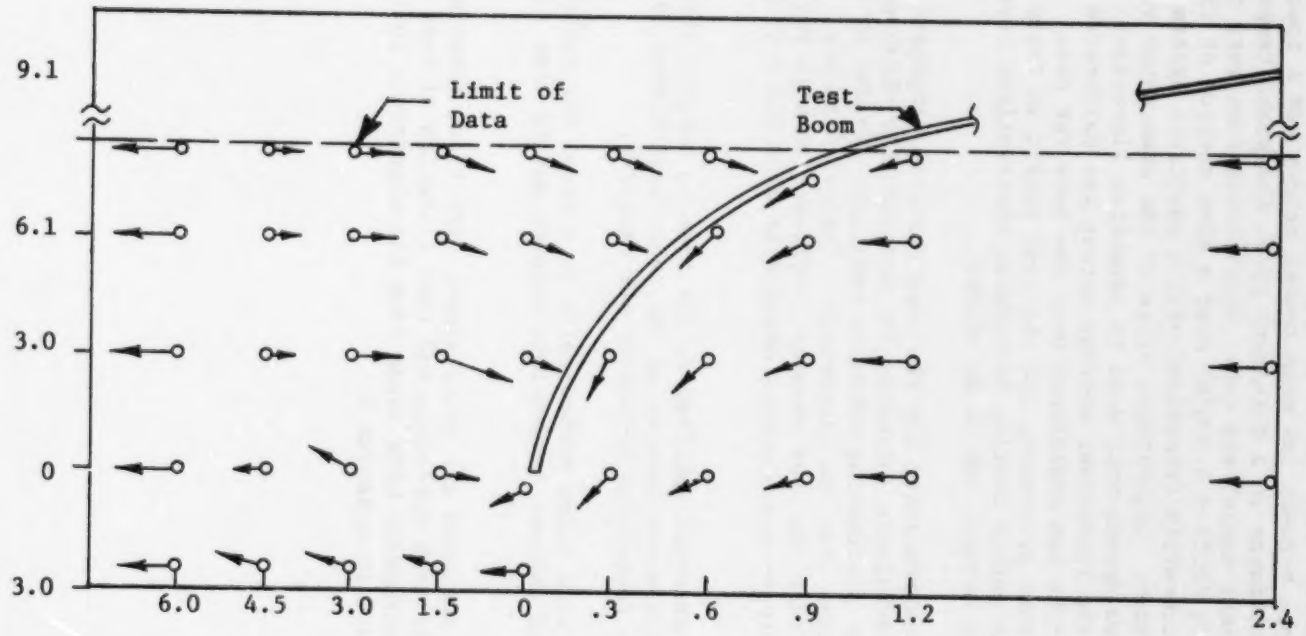

Figure 8. Schematic vector diagram of flow patterns of diversionary boom (Plan View). All measurements in meters.

were obtained without the oil slick, in salt water that was highly filtered to 30 m visibility and less than 1 ppm hydrocarbons.

Test procedures required that the boom be positioned in a diversionary mode and connected by ropes between the main towing bridge and a towable truss. With the probe positioned in a quiescent zone, the probe temperature compensation (over-heat ratio) was set. Calibration runs were then made at various tow speeds (0.25 → 1.0 m/s) over a 60-m section of the tank. Tow speeds were accurately determined with a photocell system connected to a digital timer. Logarithmic plots of the anemometer voltage outputs at various tow speeds were used to establish linearizer characteristics. After the linearizer voltage output was calibrated against tow speed, the probe was positioned near the boom for data measurements using this same procedure, and the test matrix in Table 3 was executed. During the entire testing procedure, observations were made on video tape, 16-mm movies, and 35-mm slides.

Linearizer output was monitored for the mean velocity component and the turbulence. Local turbulence intensity (%) was directly obtained as the r.m.s. voltage of the fluctuating velocity component divided by the local mean velocity voltage from the linearizer. Typical data are presented in Table 4. Since the boom changed configuration with tow speed, the closest turbulence measurements obtainable were 0.5 m from the boom.

The probe was then oriented parallel to the boom to monitor the turbulence associated with water flow along the boom (Test Number 6). No significant change in turbulence intensity was measured.

Calibration checks were taken periodically to correct for probe contamination effects and ambient temperature changes during data collection periods.

Other measurements included air (wind speed, direction, temperature) water (temperature at the tank surface), and time (duration of test run). In addition, measurements were taken from the electronic instrumentation systems as outlined in Appendix D.

TABLE 3. TURBULENCE TEST MATRIX

Tow speed, m/s	Probe position Behind	Probe position Front	Distance (x) boom to strut, m	Probe depth (z), m
0.25	x		0.305	0.101
0.25		x	0.305	0.101
0.38	x		0.610	0.101
0.38		x	0.610	0.101
0.51	x		0.915	0.101
0.51		x	0.915	0.101
0.76	x		1.22	0.101
0.76		x	1.22	0.101
0.89	x		1.52	0.101
0.89		x	1.52	0.101
1.02	x		1.83	0.101
1.02		x	1.83	0.101
0.25	x		0.305	0.304
0.25		x	0.305	0.304
0.38	x		0.610	0.304
0.38		x	0.610	0.304
0.51	x		0.915	0.304
0.51		x	0.915	0.304
0.76	x		1.22	0.304
0.76		x	1.22	0.304
0.89	x		1.52	0.304
0.89		x	1.52	0.304
1.02	x		1.83	0.304
1.02		x	1.83	0.304
0.25	x		0.305	0.660
0.25		x	0.305	0.660
0.38	x		0.610	0.660
0.38		x	0.610	0.660
0.51	x		0.915	0.660
0.51		x	0.915	0.660
0.76	x		1.22	0.660
0.76		x	1.22	0.660
0.89	x		1.52	0.660
0.89		x	1.52	0.660
1.02	x		1.83	0.660
1.02		x	1.83	0.660
0.25	x		0.305	0.406
0.25		x	0.305	0.406
0.38	x		0.610	0.406
0.38		x	0.610	0.406
0.51	x		0.915	0.406
0.51		x	0.915	0.406

(Continued)

TABLE 3. (Continued)

Tow speed, m/s	Probe position Behind	Probe position Front	Distance (x) boom to strut, m	Probe depth (z), m
0.76	x		1.22	0.406
0.76		x	1.22	0.406
0.89	x		1.52	0.406
0.89		x	1.52	0.406
1.02	x		1.83	0.406
1.02		x	1.83	0.406

TABLE 4. SELECTED TURBULENCE INTENSITY RESULTS

Test no.	Tow speed m/s (kts)	Turbulence intensity %	Probe position, m* x	y	z	Probe orientation relative to boom tow direction
1	0.72 (1.4)	2.8	2.50	0.3	0.10	Fore, $\parallel$
2	0.62 (1.2)	3.5	0.50	7.0	0.18	Fore, $\parallel$
3	0.72 (1.4)	2.4	0.50	7.0	0.10	Fore, $\parallel$
4	0.72 (1.4)	2.8	0.50	7.0	0.10	Fore, $\parallel$
5	0.72 (1.4)	2.3	0.67	17.0	0.10	Fore, $\parallel$
6	0.72 (1.4)	3.4	0.67	16.0	0.10	Fore, $\perp$
7	0.25 (0.5)	13.0	0.91	1.0	0.66	Aft, $\parallel$
8	0.56 (1.1)	14.7	0.91	0.9	0.66	Aft, $\parallel$
9	0.82 (1.6)	30.0	0.45	0.6	0.66	Aft, $\parallel$
10	0.83 (1.6)	23.6	0.60	0.6	0.66	Aft, $\parallel$
11	1.08 (2.1)	30.0	0.45	0.3	0.66	Aft, $\parallel$

*Axes Key:

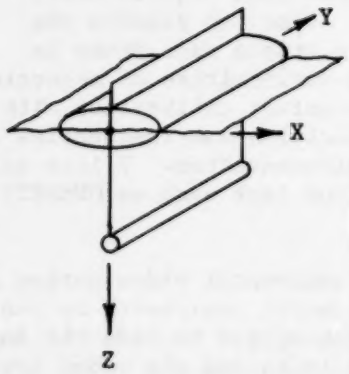

SECTION 6

DISCUSSION OF RESULTS

GENERAL DISCUSSION

Utilizing the newly developed turbulence measurement and underwater video capabilities together with flow visualization techniques, certain water flow characteristics have been identified that directly affect the performance of a diversionary boom. Carefully documented data have shown that the performance of a boom angled against a current greater than 0.5 m/s in which an oil spill is to be diverted into a collection area cannot be easily predicted from its performance head-on against the current (catenary). Consideration must be given as to how a conventional boom can be moored with numerous tie lines to maintain a nearly constant angle against the current. This should reduce the near-field turbulence and associated vortex streets that draw oil down and under the boom.

Unidirectional turbulence measurements are possible with a constant-temperature, conical, hot-film probe (DISA) at OHMSETT if the errors caused by the other two flow components are negligible and if several times each day, care is taken to check the linearizer characteristics and calibration factor for converting output voltage to velocity. Electronic and thermal noise can cause problems that require sharp filtering capabilities for their resolution. Also, to resolve the three-dimensional components of turbulence, a triple axis probe is required, which triples the complexities and difficulties of accurate measurements. Acquiring and maintaining a constant calibration with linear response over the entire range of velocities and frequencies is the main problem in using this sensitive instrumentation. Triple axis work is not likely to be feasible in an outdoor tank such as OHMSETT (5).

Development of a remotely controllable underwater video system at OHMSETT greatly enhances testing oil spill control equipment, as was demonstrated here. Future improvements to the system include the installation of traveling rail systems for the video truss and the video tow strut to allow complete coverage between the main and auxiliary bridges.

Previous tests (none of this type were conducted here) have shown a tremendous variation in boom performance with oil properties, especially specific gravity (7). This property was not varied during the test project.

EPA has sponsored several fast current boom development projects in

the past that have demonstrated to some extent the ability to design booms for hydrodynamic smoothness and associated turbulence reduction (2, 3). We hope that this work will assist future boom development projects aimed at improving oil spill control capabilities for a cleaner environment.

TEST TANK EFFECTS ON DATA

Test tanks can only approximate actual waterways. There is no real current, except with flumes. A separate report would be needed to rigorously define all of the differences, but the primary one that affected this test project was that the currents are simulated by the relative motion of the traveling bridge with respect to "motionless water." In effect, the velocity profiles horizontally across the tank (wall to wall) and vertically from the water surface to the tank bottom are flat and that the background turbulence is zero except for disturbances due to convection, the wind, or the previous test run. As a result, the background turbulent intensity is not a fixed value but varies inversely with tow speed. However, typical river velocity profiles are generally considered to be parabolic from shore to shore and approximately linear from bottom (where current is zero) to water surface (maximum current). For some rivers with very steep banks, the surface velocity profile becomes nearly flat. But for most cases, when the diversionary technique is being applied, the very reason for setting the boom at a smaller angle with the mid-stream current is to prevent those currents greater than 0.5 m/s from directly encountering the boom and causing oil loss. Ideally, the fast mid-stream currents are used to divert oil to the much slower current zone near the shoreline. When testing this concept in the test tank, obviously there was no "slow current" zone. The bridge moves with respect to the tank water, and this relative velocity is the same all across the tank.

How does this affect the correlation of diversionary boom performance in the test tank and the real world? Boom failure inadvertently occurred at the trailing end which was angled the most against the current and should have been in the "quiet zone" (that does not exist in a test tank). If a "quiet zone" did exist near the test tank wall (or trailing edge of the boom), the "no oil loss" test speed would have increased and been in closer agreement with actual performance in waterways with parabolic surface velocity profiles and "quiet zones." The result is that the diversionary "no oil loss" tow speeds are low and conservative. However, as shown by the results of this work, other difficulties and water flow complexities contribute to the performance level too.

REFERENCES

1. Bradshaw, P.:1971, An Introduction to Turbulence and Its Measurement, Pergamon Press, New York.

2. Dorrler, J.S., Ayers, R., and Wooten, D.C.:1975, High current control of floating oil. In: Proceedings of Joint Conference on Prevention and Control of Oil Spills. Washington, D.C.: American Petroleum Institute.

3. Folsom, B.A.:1975, Development of a streamlined oil retention boom. Unpublished interim report for the U.S. Environmental Protection Agency, Office of Research and Development, Cincinnati, O. Ultrasystems Contract No. 68-03-0403, December 1975.

4. Freestone, F.J., McCracken, W.E., and Lafornara, J.P.:1976, Performance testing of spill control devices on floatable hazardous materials. In: Proceedings of National Conference on Control of Hazardous Material Spill. Information Transfer, Inc., Rockville, Maryland.

5. Hale, L.A., Norton, D.J., and Rodenberger, C.A.:1974, The Effects of Currents and Waves on an Oil Slick Retained by a Barrier. U.S. Coast Guard, Office of Research and Development, Washington, D.C. Report No. CG-D-53-75.

6. Hires, R.I.:1976, Some Comments on the Use of Hot Film Anemometry at EPA OHMSETT Facility. Stevens Institute of Technology, Davidson Laboratory: Technical Note 878.

7. McCracken, W.E.:1977, Performance Testing of Selected Inland Oil Spill Control Equipment. U.S. Environmental Protection Agency, Office of Research and Development, Cincinnati, O. Report No. EPA-600/2-77-150, August 1977.

8. Warschauer, K.A., Vijge, J.B.A., and Boschloo, G.A.:1974, Some experiences and considerations on measuring turbulence in water with hot films. Applied Scientific Research: 29. April 1974.

9. Wicks, M.:1969, Fluid dynamics of floating oil containment by mechanical barriers in the presence of water currents. Proceedings of Joint Conference on Prevention and Control of Oil Spills, Washington, D.C.: American Petroleum Institute.

10. Wilkinson, D.L.:1972, Dynamics of contained oil slicks. In: Proceedings of the American Society of Civil Engineers, Journal of the Hydraulics Division. June 1972, pp. 1013-1030.

APPENDICES

APPENDIX A. OHMSETT DESCRIPTION

Figure A-1. OHMSETT.

The EPA OHMSETT facility provides an environmentally safe place to conduct testing and development of devices and techniques for the control of oil and hazardous materials spills.

The primary feature of the facility is a pile-supported, concrete tank with a water surface 203.3 m long by 19.8 m wide and with a depth of 2.44 m. The tank can be filled with either fresh or salt water. The tank is spanned by a towing bridge with a capability of towing loads up to 15422.4 kg at speeds to 3.05 m/s for a duration of 45 s. Slower speeds yield longer test runs. The towing bridge is equipped to lay oil on the surface of the water several feet ahead of the device being tested, such that reproducible thicknesses and widths of oil slicks can be achieved with minimum interference by wind.

The principle systems of the tank include a wave generator and beach, a bubbler system, and a filter system. The wave generator and absorber beach have capabilities of producing minimum reflection waves up to 0.8 m high and 36.6 m long, as well as a series of reflecting, complex waves meant to simulate the water surface of a harbor or estuary. The water is clarified by recirculation through a 1.26 m^3/s, diatomaceous earth filter system to permit underwater photography and video imagery

and to remove the hydrocarbons that enter the tank water as a result of testing. Oil is controlled on the surface of the water by a bubbler system that prevents oil from reaching the tank walls, the beach, or the wave generator. This system is designed to speed the clean up between test runs, since a clean tank surface is essential to reproducible oil spill conditions. The towing bridge has a built-in skimming board that, in conjunction with the bubbler system, can move oil on to the north end of the tank for cleanup and recycling.

When the tank must be emptied for maintenance purposes, the entire water volume (9842 m^3) is filtered and treated until it meets all applicable State and Federal water quality standards before being discharged. Additional specialized equipment will be used whenever hazardous materials are used for tests. One such device is a trailer-mounted carbon treatment unit that is available for removal of organic materials from the water.

Tests at the facility are supported from a 650-m^2 building adjacent to the tank. This building houses offices, a quality control laboratory (which is very important since test oils and tank water are both recycled), a small machine shop, and an equipment preparation area.

This government-owned, contractor-operated facility is available for testing purposes on a cost-reimbursable basis. The operating contractor, Mason & Hanger-Silas Mason Co., Inc., provides a staff of 11 multi-disciplinary personnel. EPA provides expertise in the area of spill control technology, and over all project direction.

For additional information, contact:

OHMSETT Project Officer
U.S. Environmental Protection Agency
Office of Research and Development
Edison, New Jersey 08817
Phone: 201-321-6631

APPENDIX B. UNDERWATER VIDEO

To examine effectively the three-dimensional flows of water and oil around the diversionary boom, it was necessary to select an underwater video system capable of resolving the entrained oil droplets. This was done in a two-part test series: a target series using a resolution target (Figure 3) and a bead series using plastic beads as an oil simulant. Two camera systems were used for comparison-- one system borrowed from the Navy Ship Research and Development Center (the NSRDC fish) in Bethesda, Maryland; and the other (the EPA fish), an IVC-40 M 850 line, high resolution camera with a standard visible light band vidicon and remotely controlled focus, iris, and zoom.

The tests were conducted to determine the following capabilities:

1) Resolution with and without underwater lights.

2) Differences in performance of a faired camera housing (NSRDC camera) and an unfaired cylindrical camera housing (EPA) under tow up to 3.0 m/s.

3) Wide field of vision using either a rotatable mirror aligned with the camera (NSRDC) or externally rotating and tilting the camera and canister.

The EPA fish and NSRDC fish were mounted near each other and positioned so that each would have approximately the same lighting depth, water conditions, and viewing angle. Visibility in this case was defined as the distance an object could be sharply seen by the human eye through the test tank window. Ambient light readings were taken in foot candles, 1.8 m above the camera with a Spectra Pro meter using an incident dome. Resolution was defined as follows: 1) Good: sharp, clean lines; 2) Fair: slight blur, but distinguishable lines; 3) Poor: very blurred, undistinguishable lines.

During the course of resolution testing, observations were made of related conditions. In relation to viewing angles, zoom, pan, and tilt were found to be essential to find and view the object properly. Even a slight target movement because of waves or tow forces meant loss of image or major time delays if the field of view was not changed. Although the zoom, pan, and tilt motions were very useful, the movements appeared to be sluggish.

Three different types of distortion were discerned. Distortion resulting from camera and target motion was noticeable at 0.51 m/s as a small shadow movement, but it did not distract from the picture image significantly. Distortions resulting from the pan and tilt assembly were of two types: (a) primary distortion, caused where the field of vision became larger than the rotatable mirror, was a shaded area or double image; and (b) secondary distortion, a result of viewing objects at sharp angles, was elongated images.

The interaction of the controls (zoom, focus, and iris) at low light conditions required excessive amounts of time for focusing. The smaller the iris, the easier the image was to focus. Reducing the iris size was accomplished by increasing the light entering the camera or by increasing the camera's sensitivity electronically.

The procedure followed in the testing program began by positioning both cameras and the resolution chart. After checking out the electronics, ambient conditions were recorded; these included wind speed and direction, air and water temperature, water surface condition, cloud cover, and tank water visibility. Test conditions such as waves, lighting, or tow speed were established before recording resolution, depth of field, and other general observations.

Before testing began, a section of the tank bottom was vacuumed to remove dark layers of sediment and expose the white paint below. Light meter readings taken 5.1 cm above the surface of the water in a reflective mode indicated that the foot candle readings increased from 2368.1 lux (lx) over the dirty bottom to 10763.9 lx over the clean bottom. Although the cleaned area was narrow (1.8 m), a significant increase in picture quality was noticed when the camera passed through this area.

Each camera's viewing area was somewhat limited in maneuverability. The NSRDC camera could be rotated and tilted, but not zoomed. The EPA fish could be zoomed, but its viewing angle could not be varied. To standardize the test, the NSRDC camera was positioned at approximately the same angle as the EPA fish, which was then zoomed to approximately the same magnitude as the NSRDC camera. Since the NSRDC camera had no lights of its own, the EPA lights were used to illuminate its target; but it should be noted that there was an additional 0.6 m for the EPA light to travel to the NSRDC target. The entire camera and mirror assembly was controlled above water. For detailed descriptions of the equipment used in the testing program, refer to Appendix D.

As a result of these tests and studies, the underwater video system was designed with the following characteristics:

1) The IVC 40 M camera was determined to have adequate resolution capabilities (0.3-cm beads at 6.0 m) with ambient light (≃ 2152.8 lx), highly filtered water, and a clean, white tank bottom.

2) An external pan and tilt unit with remote control was attached to the cylindrical canister at the end of a faired tow strut.

The video camera tow strut is shown in Figure 4, mounted to the auxiliary bridge.

APPENDIX C. B.F. GOODRICH SEA BOOM

Design Characteristics

1. Draft--0.30 m
2. Freeboard--0.15
3. Flotation--continuous chambers of closed-cell foam, protected by 0.635-cm PVC coating and secured at the boom ends with wooden plugs.
4. Ballast--tubular extrusions filled with lead shot and sand.
5. Skirt material--0.635-cm-thick vinyl sheet reinforced with rib handles of urethane.
6. Tension member--self-tensioning boom.
7. Weight--11.92 kg/m
8. Excess buoyancy--10.42 kg/m
9. Standard length--7.16 m

Tow Point Connection

1. A bridle arrangement was connected to the manufacturers-provided SEALOC system. This consists of a piano hinge arrangement with fiberglass pins.

Comments

1. Required 10 men/section for handling (as well as crane for deployment and removal).
2. End plates and connections were easy.

APPENDIX D. TEST EQUIPMENT

The following section of this report describes the electronic instrumentation used for hot film turbulence measurements. Figure D-1 depicts each instrument and its position in the instrumentation set-up. Individual systems are detailed in the following manner:

Manufacturer: Name of system
Description of equipment
Technical Data

Certain materials are reprinted courtesy of the individual manufacturers.

DISA Conical Hot Film Probe

The probe used during the testing was a conically shaped probe with a thin nickel film placed around the tip of the cone. The sensor was thinly coated with quartz to protect the metal film against ambient influences; sensors for use in electrical conducting liquids are coated to a thickness of approximately 2μm to be secured against breakthrough and against electrolysis of the nickel film.

The particular advantage of the conical configuration of this probe is its insensitivity to mechanical contamination, since dirt particles will not readily stick to it because of its pointed shape.

Technical data:

Sensor dimensions: 1.4 mm x 0.1 mm
Sensor resistance: 15Ω
Maximum sensor temperature: 150°C
Maximum ambient temperature: 100°C
Minimum velocity: 0.01 m/s
Maximum velocity: 25 m/s
Frequency limit: (F_{CMAX}): 30 kHz

DISA Electronics 55D01 Anemometer

The constant-temperature anemometer measurements are based on balancing the convective heat loss as a result of the mass flow around the hot film probe.

The unit consists of a Wheatstone bridge and an amplifier. Specifications are available from DISA Electronics, Franklin Lakes, New Jersey.

DISA Electronics 55D10 Linearizer

The linearizer performs the function of canceling the anemometer output voltage corresponding to no-flow probe output and raising the output voltage by a suitable exponent. The linearizer transfer function results in a voltage that varies directly as the flow velocity so that

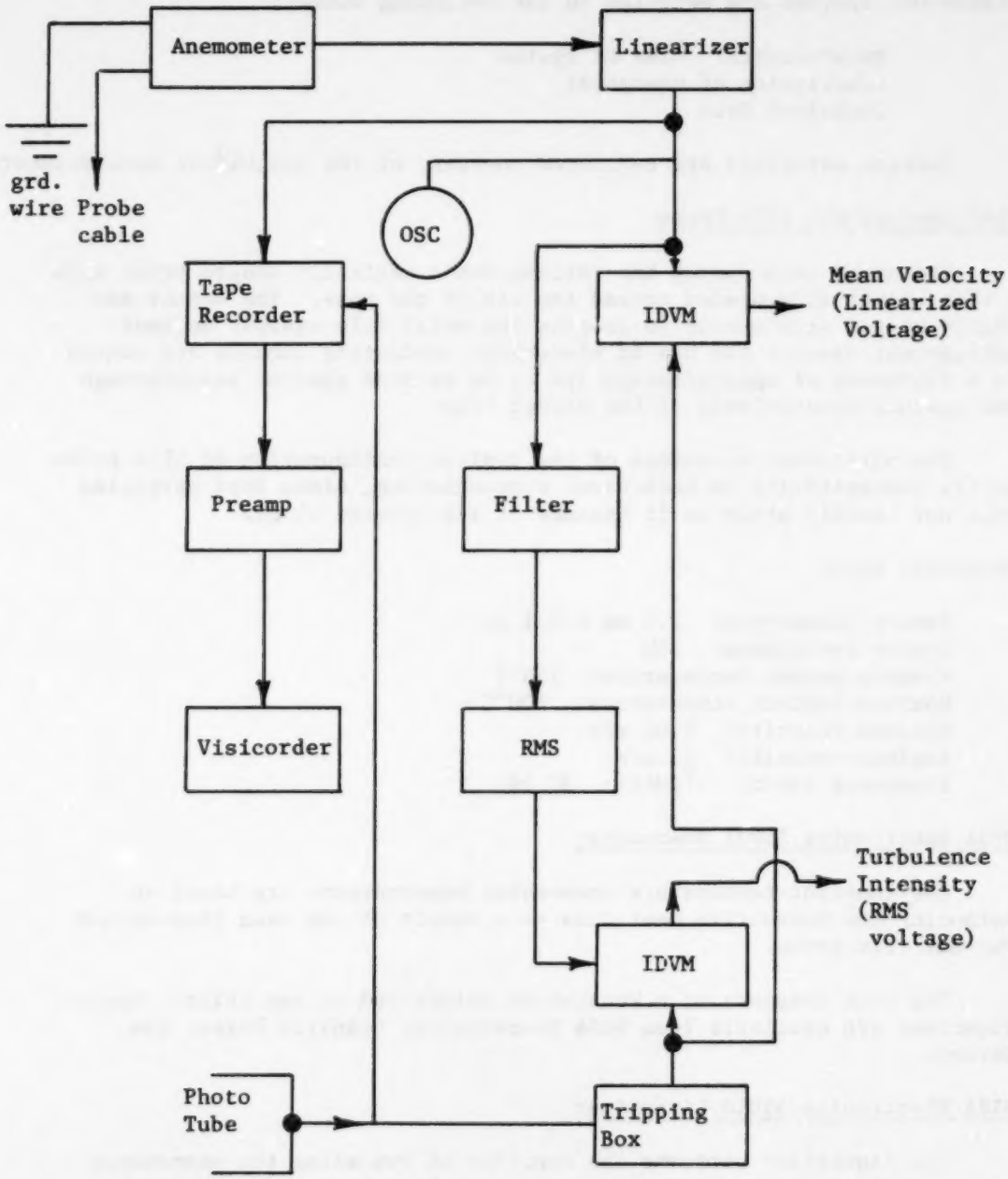

Figure D-1. Instrumentation diagram for single-axis probe.

the calibration curve starts at the origin of the system of co-ordinates, reaching approximately 10 volts for the highest velocity occurring in practice. A feature of the linearizer is that it uses logarithmic amplifiers to provide optimum linearization throughout the range. In this way, continuous linearization of the anemometer output voltage is obtained. In other words, the same order of linearization accuracy is obtained for any voltage within the range in question.

Technical data:

Accuracy: Linearization on the order of 0.5% to 3% can be accomplished, depending on conditions of measurement
Output voltage range: 0 to 10 volts
Frequency range: 0 to 100 kHZ at output voltage 5 volts and exponent m = 2.0
Output impedance: 180 Ω
Power supply: 100/220 volts ±10%, 50 to 60 Hz
Input impedance: 6.8 kΩ to 28 kΩ, continuously adjustable

DISA Electronics 55D25 Auxiliary Unit

This auxiliary unit converts the output signal of the anemometer or linearizer into a form suitable for further processing by other instruments. For this purpose, it incorporates an amplifier, switchable filters, and a square-wave generator for making the anemometer square-wave test.

Technical data:

Gam: calibrated 1, continuously variable from 1 to approximately 3.
Frequency range: D.C. to 500 kHz
Input impedance: Approximately 16 kΩ
Output impedance: Approximately 160 Ω
High pass filter: 11 positions DC 1-1000 Hz
Low pass filter: 11 positions 0.2-200 kHz

DISA Electronics 55D35 RMS Voltmeter

The voltmeter measures the true root means squared (RMS) values of AC voltages in the wide range from 300μV to 300 volts. When used with an anemometer, its chief application is the determination of the dynamic components of flows.

Readout was provided by an accuracy meter. External indication was also possible via a BNC socket. The RMS voltmeter had an additional output socket at which the squared RMS value of the AC voltage under measurement was available. This output was used for determining the turbulence energy spectra of flows.

Technical data:

Full-scale ranges: 1 mV to 300 Volts
Accuracy of RMS output at mid-range frequencies: ±1% of maximum

output voltage, down to -30dB.
Accuracy of squared RMS output at mid-range frequencies: ±1% of maximum output voltage, down to -30dB.

APPENDIX E. TEST PROCEDURE FOR TURBULENCE MEASUREMENT

Manpower Allocations

The following allocations of duties were made:

1. Test director--responsible for running the tests according to the prescribed test matrix and test procedure; manages the test personnel.

2. Control room operator--operates the traveling bridge from the control tower at the north end of the tank. He also collects the data for ambient conditions.

3. Photographer--photographically documents the test runs with 35 mm color slides, 16-mm color motion pictures, and the underwater video system.

4. Data documentation technician--records test data and follows directions of test director.

Pre-test Checklist

To ensure that all test systems and equipment were maintained and ready for the test day, the following checklist was used before the first test run:

1. Bridge drive system operating.

2. Test device operational.

3. Test instrumentation operational.

4. Test support equipment operational.

5. Photographic systems ready.

6. Test personnel prepared and ready.

7. All pre-run data and checklists completed.

Test Sequence

The following test sequence was used for the hot-film probe turbulence tests:

1. Position the traveling bridge and test devices for testing.

2. Position all personnel for testing.

3. Inform all test personnel of test conditions taken from the test matrix.

4. Set probe controls and energize probe by switching to operational mode from standby mode.

5. Give three blasts on the air horn to clear the tank and alert all test personnel of test run.

6. Using either an intercom system or walkie-talkies, begin a countdown from five with the control room operator to begin bridge motion at zero and one blast on the air horn.

7. Initiate the bridge movement and photographic documentation with one blast on the air horn.

8. Record test data during test run (data documentation technician).

9. Begin countdown from five to stop the bridge (test director).

10. Return bridge and boom to starting point and prepare for the next test.

Data Analysis

The test director performed all data analysis and reduction. All data sheets were submitted to him for compilation onto master raw data sheets as shown in Appendix F. The ultimate responsibility for proper data collection, analysis, and presentation belongs to the OHMSETT project engineer, who writes the final report for the EPA project officer.

Conical-Type Hot Film Probe Procedures

1. The probe was turned on and sufficient warm-up time allowed.

2. Controls were set as follows:

   A. Meter switch to 10.
   B. Decade resistance to 00.00.
   C. Loop control at standby.
   D. Bridge ratio at 1:20.
   E. Gain adjustment at 3.
   F. Temperature--resistance switch at neutral.

3. The probe support and shorting probe were attached by a 5-m probe scale.

4. The shorting probe was replaced with an actual probe. The decade resistance was set to a value that gave no meter deflection when the temperature resistance switch was set.

5. Resistance was noted on the decade box, and this value was multiplied by 1.1 (operating resistance for correct operation was determined by the overheat factor, which could not exceed 1.1 times the ambient resistance of the probe).

Probe sensor resistance = R_{Temp}
Leads resistance = $R_{0.9}$
$(R_{Temp} - R_{0.9})\ 1.1 + R_{0.9}$ = Operation resistance

6. Appropriate operating resistance was set.

7. The probe was energized by switching to operation mode from standby mode.

8. Voltage outlet from the probe was observed and noted.

9. Readings at zero speed of the output voltage E were taken from the anemometer.

10. E_B (Bridge anemometer output voltage) was integrated over 60.9 m for the following tow speeds (u):

0.25 m/s	0.76 m/s
0.38	0.89
0.51	1.02
0.64	Repeat stationary

11. The following formula was used to calculate the exponent which was plotted as stated (see p. vii for definitions of abbreviations and symbols).

$$\ln [(E_B/E_0)^2-1] \text{ vs } \ln u$$

12. The fictive zero was set if necessary to ensure an adequate linear relationship.

$$\ln [(E_B/.9E_0)^2-1] \text{ vs } \ln u \text{ on linearizer.}$$

13. The exponent determined from the previous plot was set.

14. Temperature compensation was set.

15. With the probe at zero speed and the fictive voltage output from the anemometer, the zero adjust was set to zero output from the linearizer.

16. Towing the probe at highest speed (1.27 m/s), the gain adjust was set on the linearizer to obtain a 5-volt output.

17. Towing at half the highest speed (0.64 m/s) produced approximately 2.5 volts. When the exponent was changed, the temperature compensation was adjusted again.

18. During calibration runs, the RMS output was recorded by reading the scale; setting the time constant to 10 s produced steady readings. For example, 1% turbulence gave 0.05 V RMS when the mean lineage output was 5 volts.

APPENDIX F. PRESENTATION OF TEST RESULTS

The following test results tables list the ambient conditions during testing, probe positions, and linearizer output for each individual test. The results-oriented individual will be most interested in the "Intensity RMS/Auxiliary" column, since this is the actual measure of turbulent intensity encountered by the probe in its various positions around the boom. The Auxiliary voltage (V) is a measure of the linearizer output, the RMS voltage (V) being the treated signal of the linearizer output.

TABLE F-1. (Continued)

Test no.	Date	Wind speed m/s	Wind dir.	Air temp. °C	Tow speed m/s	Auxiliary (V)	RMS full scale	RMS (V)	Intensity RMS/Aux.	Probe position, m* x	y	z	Probe relative to boom	Comments
34	4/16	3.35	WNW	29.0	0.540	0.13	0.1	0.81	62.31	1.06	0.91	3.50	Aft	No filter
35	4/16	3.35	WNW	29.0	0.540	0.14	0.1	0.82	58.57	1.06	0.91	3.50	Aft	No filter
36	4/16	3.35	WNW	29.0	0.550	1.22	0.1	0.20	1.64	1.50		0.66	Aft	
37	4/16	3.35	WNW	29.0	1.070	1.78	0.1	0.19	1.07	1.50		0.66	Aft	
38	4/16	3.35	WNW	29.0	0.270	0.60	0.1	0.29	4.83	1.50	1.80	0.66	Aft	
39	4/16	3.35	WNW	29.0	0.540	1.15	0.1	0.19	1.65	1.50		0.66	Aft	
40	4/16	3.35	WNW	29.0	1.070	1.73	0.1	0.20	1.16	1.50		0.66	Aft	
41	4/16	3.35	WNW	29.0	0.280	0.64	0.1	0.09	1.41	1.20	1.80	0.66	Aft	
42	4/16	3.35	WNW	29.0	0.540	1.24	0.1	0.40	3.23	0.91	0.91	0.66	Aft	
43	4/16	3.35	WNW	29.0	0.290	0.86	0.1	0.20	2.33	1.30	1.06	0.66	Aft	
44	4/16	3.35	WNW	29.0	1.060	1.77	0.1	0.51	2.88	1.50	0.76	0.66	Aft	
45	4/19	0.44	SE	22.0	1.060	1.12	0.003	0.98	0.30	0.73	0.30	0.30	Fore	
45R	4/19	0.44	SE	22.0	1.050	1.11	0.01	0.04	0.04	0.73	0.30	0.30	Fore	
45R[2]	4/19	4.24	WNW	30.0	1.050	1.12	0.003	0.13	0.03	0.73	0.30	0.30	Fore	
45R[3]	4/19	4.24	WNW	30.0	1.010	1.05	0.003	0.18	0.05	0.73	0.30	0.10	Fore	
46	4/19	5.27	NNW	32.0	1.050	1.08	0.003	0.18	0.05	0.73	0.30	0.66	Fore	
47	4/19	3.35	NNW	32.0	1.060	1.05	0.003	0.23	0.06	2.40	0.30	0.66	Fore	
47R	4/19	3.35	NNW	32.0	1.050	1.05	0.003	0.21	0.06	2.40	0.30	0.66	Fore	
48	4/19	3.35	NNW	32.0	1.050	1.04	0.003	0.22	0.06	2.40	0.30	0.30	Fore	
48R	4/19	3.35	NNW	32.0	1.040	1.04	0.003	0.21	0.06	2.40	0.30	0.30	Fore	
49	4/19	5.27	NNW	32.0	1.050	1.03	0.003	0.22	0.06	2.40	0.30	0.10	Fore	
49R	4/19	3.35	NNE	33.0	1.040	1.02	0.003	0.23	0.07	2.40	0.30	0.10	Fore	
50	4/19	3.35	NNE	33.0	1.030	1.03	0.003	0.16	0.05	2.10	0.76	0.10	Fore	
50R	4/19	3.35	NNE	33.0	1.030	1.02	0.003	0.18	0.05	2.10	0.76	0.10	Fore	With filter
51	4/19	3.35	NNE	33.0	1.050	0.98	0.003	0.22	0.06	2.10	0.76	0.30	Fore	With filter
51R	4/19	3.35	NNE	33.0	1.050	2.07	0.03	0.46	0.67	1.98	0.76	0.30	Fore	With filter
52	4/19	3.35	NNE	33.0	1.050	2.12	0.03	0.48	0.68	1.98	0.76	0.66	Fore	With filter
53	4/19	3.35	ENE	33.0	1.040	0.78	0.03	0.30	1.15	1.98	0.76	0.10	Fore	With filter
53R	4/19	3.35	ENE	33.0	1.040	0.74	0.03	0.35	1.42	1.98	0.76	0.10	Fore	With filter
54	4/19	3.35	ENE	33.0	1.030	0.70	0.03	0.27	1.17	1.60	0.60	0.10	Fore	With filter

(Continued)

TABLE F-1. (Continued)

Test no.	Date	Wind speed m/s	Wind dir.	Air temp. °C	Tow speed m/s	Auxiliary (V)	RMS full scale	RMS (V)	Intensity RMS/Aux.	Probe position, m* x	y	z	Probe relative to boom	Comments
55	4/19	3.35	ENE	33.0	1.040	0.70	0.03	0.26	1.11	1.60	0.60	0.30	Fore	With filter
56	4/19	3.35	ENE	33.0	1.050	0.79	0.03	0.25	0.95	1.60	0.60	0.66	Fore	With filter
56R	4/19	3.35	ENE	32.5	1.060	0.76	0.03	0.22	0.88	1.60	0.60	0.66	Fore	Dye included
57	4/19	3.35	ENE	32.5	1.060	0.78	0.03	0.21	0.81	1.31	0.60	0.66	Fore	Dye included
57R	4/19	3.35	ENE	32.5	1.060	0.76	0.03	0.23	0.92	1.31	0.60	0.66	Fore	Dye not included
58	4/19	3.35	ENE	32.5	1.080	0.72	0.03	0.22	0.92	1.31	0.60	0.30	Fore	With filter
59	4/19	3.35	ENE	32.5	1.070	0.69	0.03	0.22	0.94	1.31	0.60	0.10	Fore	With filter
60	4/19	3.35	N	31.0	1.070	0.68	0.03	0.24	1.04	1.21	0.60	0.10	Fore	With filter
61	4/19	3.35	N	31.0	1.070	0.71	0.03	0.23	0.96	1.21	0.60	0.30	Fore	With filter
62	4/19	3.35	N	31.0	1.060	0.78	0.03	0.21	0.81	0.91	0.60	0.66	Fore	With filter
63	4/19	3.35	N	31.0	1.070	0.79	0.03	0.23	0.86	0.91	0.60	0.66	Fore	With filter
64	4/19	3.35	N	29.0	1.070	0.72	0.02	0.24	1.00	0.91	0.60	0.30	Fore	With filter
65	4/19	3.35	N	29.0	1.060	0.68	0.03	0.27	1.19	0.91	0.60	0.10	Fore	With filter

*x-Distance from strut to center of boom
y-Distance from strut to end of boom.
z-Probe depth.

**See Table 4 for axes key.

TABLE F-1. TEST RESULTS

Test no.	Date	Wind speed m/s	Wind dir.	Air temp. °C	Tow speed m/s	Auxiliary (V)	RMS full scale	RMS (V)	Intensity RMS/Aux.	Probe position, m* x	y	z	Probe relative to boom	Comments
1	3/15	6.71	NW	8.3	0.555	2.02	0.3	0.322	4.78	0.61	1.27	0.30	Fore	
2	3/15	6.71	NW	8.3	0.427	1.88	0.3	0.395	6.30	0.45	1.27	0.30	Fore	
3	3/15	6.71	NW	8.3	0.552	2.01	0.3	0.340	5.07	0.61	1.01	0.30	Fore	
4	3/15	6.71	NW	8.3	0.552	2.25	0.3	0.810	10.80	1.77	1.06	0.39	Fore	
5	3/15	4.47	ESE	3.3	0.549	3.94	1.0	0.430	10.91	1.82	0.91	0.39	Fore	
6	3/15	4.47	ESE	3.3	0.555	9.54	1.0	0.790	8.28	1.82	1.06	0.39	Fore	
7	3/15	3.58	ENE	1.7		1.10						0.39	Fore	
8	3/15	4.02	NW	7.2	0.555	1.85	1.0	0.240	12.97	12.75	**	0.39	Fore	
9	3/15	4.02	NW	7.2	0.555	2.18	1.0	0.320	14.68	12.75	**	0.39	Fore	
10	3/15	6.71	WNW	10.0	0.826	3.38	1.0	0.320	9.47	12.75	**	0.39	Fore	
11	3/15	4.47	WNW	13.3	1.064	4.05	1.0	0.270	6.67	12.75	**	0.39	Fore	
12	4/14	2.67	WNW	16.0	0.280	0.27	0.3	0.250	27.78	0.76		0.66	Aft	No filter
13	4/14	3.35	WNW	17.0	0.540	0.74	0.3	0.300	12.16	0.60	1.06	0.66	Aft	No filter
14	4/14	3.35	WNW	17.0	0.420	0.46	0.3	0.280	18.26	0.76	1.20	0.66	Aft	No filter
15	4/14	3.35	WNW	17.0	0.540	0.60	0.3	0.280	14.00	0.45	1.06	0.66	Aft	No filter
16	4/14	3.57	WNW	17.0	0.400	0.32	0.3	0.300	28.13	0.76	1.30	0.66	Aft	No filter
17	4/14	3.57	WNW	17.0	0.280	0.20	0.3	0.180	27.00	1.06	1.60	0.66	Aft	No filter
18	4/14	3.57	WNW	17.0	0.810	1.86		0.930	R U N	A B O R T E D				
18R	4/14	3.57	WNW	17.0	0.810	1.77	1.0	0.370	20.90	0.91	0.76	0.66	Aft	No filter
19	4/14	3.57	WNW	17.0	0.890	1.85	1.0	0.310	16.76	0.60	4.50	0.66	Aft	No filter
20	4/14	3.35	NW	18.0	1.070	1.94	1.0	0.350	18.04	0.76	4.50	0.66	Aft	No filter
21	4/14	3.35	NW	18.0	0.800	1.54	1.0	0.330	21.43	0.76	0.76	0.66	Aft	No filter
22	4/16	1.34	NW	26.0	0.560	0.97				4.50		0.66		Calibrate
23	4/16	1.34	NW	26.0	1.090	1.48				4.50		0.66		Calibrate
24	4/16	1.34	NW	26.0	0.820	1.20				4.50		0.66		Calibrate
25	4/16	1.34	NW	26.0	0.280	0.48				4.50		0.66		Calibrate
26	4/16	1.34	NW	26.0	0.270	0.23	0.3	0.100	13.04	0.91	1.06	0.66	Aft	No filter
27	4/16	1.34	NW	26.0	0.550	0.55	0.3	0.270	14.73	0.91	0.91	0.66	Aft	No filter
28	4/16	1.34	NW	26.0	0.830	0.39	0.3	0.390	30.00	0.45	0.60	0.66	Aft	No filter
29	4/16	1.34	WNW	26.0	0.830	0.47	0.3	0.370	23.62	0.60	0.60	0.66	Aft	No filter
30	4/16	3.35	WNW	29.0	1.080	0.40	0.3	0.400	30.00	0.45	0.30	0.66	Aft	No filter
31	4/16	3.35	WNW	29.0	0.280	0.75	0.1	0.300	4.00	0.91	1.80	3.50	Aft	No filter
32	4/16	3.35	WNW	29.0	0.550	0.63	0.1	0.840	13.33	0.91	0.9	3.50	Aft	No filter
33	4/16	3.35	WNW	29.0	R U N	A B O R T E D								No filter

(Continued)